Keele University

STAREX, Sierre, Oct 2021

KAVLI IPMU

erc
European Research Council
Established by the European Commission

PRACE

321D: the case of entrainment

Raphael HIRSCHI
Keele University, UK

SHEN @ Keele: L. Scott, E. Kaiser, F. Rizzuti
in collaboration with:
BHs: K.Belczynski (NCAC, Pl), J. Groh, E. Farrel (TCDublin, Ie)
GVA code: G. Meynet, A. Maeder, C. Georgy, S. Ekström, P. Eggenberger, A. Choplin and C. Chiappini (IAP, D)
VMS: N. Yusof, H. Kassim (UM, KL, Malaysia), P. Crowther (Sheffield), O. Schnurr (IAP)
Nucleo: F.-K. Thielemann, U. Frischknecht, T. Rauscher (Basel, CH/Herts, UK) N. Nishimura (Riken, Jp)
NUGRID: F. Herwig (Victoria, Canada), M. Pignatari (Hull), C. Fryer, S. Jones (LANL),
J. den Hartogh (Konkoly Obs., H), Laird (York), U. Battino (Edinburgh), UChicago, UFrankfurt, …
SNe: K. Nomoto (IPMU, J), C. Frohlich, M. Gilmer (NCSU), A. Kozyreva (MPA, D), T. Fischer (Wroclaw,Pl)
HYDRO: C. Meakin, D. Arnett (UArizona), C. Georgy (GVA), M. Mocak
F. Roepke, L. Horst (HITS, D), S. Jones (LANL, US), P. Edelmann (LANL, US)

DiRAC

ChETEC Action

Keele is Not Kiel (Germany) But Where is it?

West Midlands:

Keele area

is famous for pottery: Wedgwood, ...

Exciting HyDeploy.co.uk / SEND projects

Plan

- 321D concept

- Entrainment:

    3D results

    Theory

    1D implementation

    1D results: MS width, core masses, …

- Boundary shape - shear

- Conclusions & Outlook

Way Forward: 1 to 3 to 1D link

Targeted 3D simulations

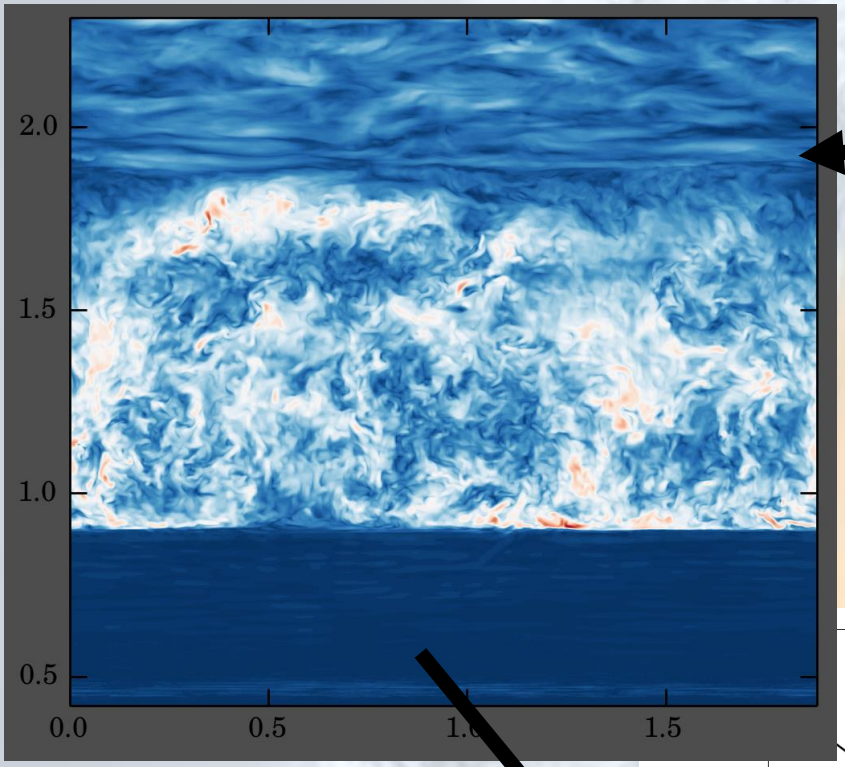

Cristini+2017

Uncertainties in 1D

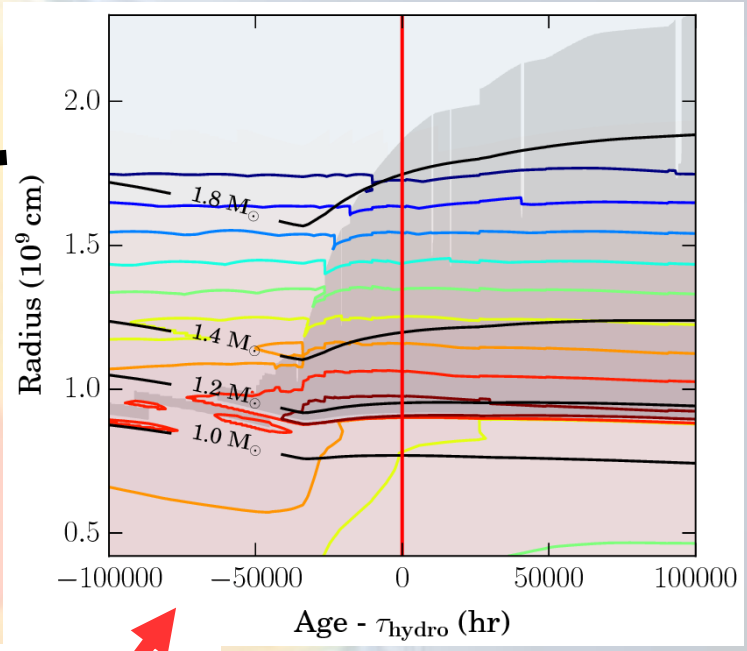

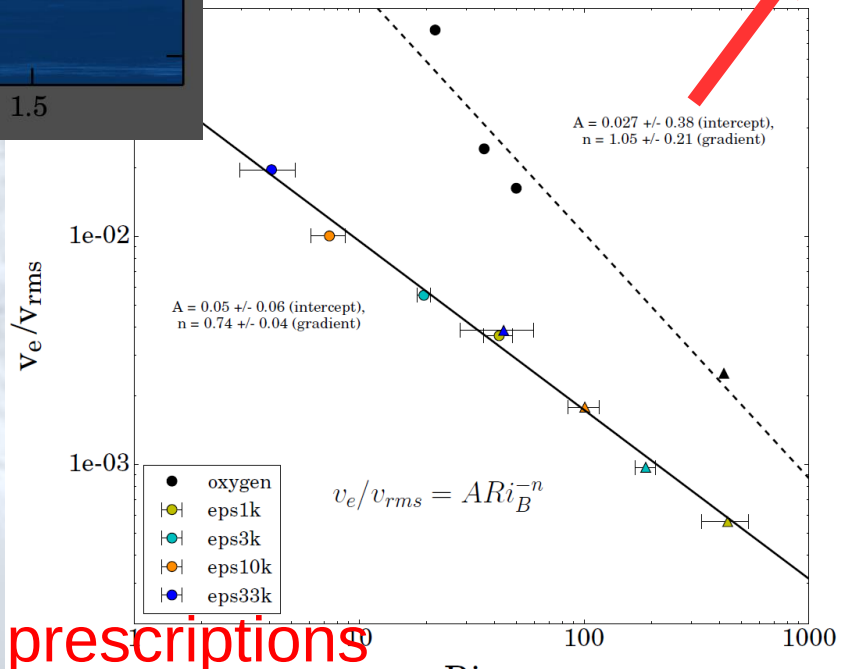

→ Improve theoretical prescriptions

3D C-shell Simulations

Snapshot from 1024^3 resolution run:

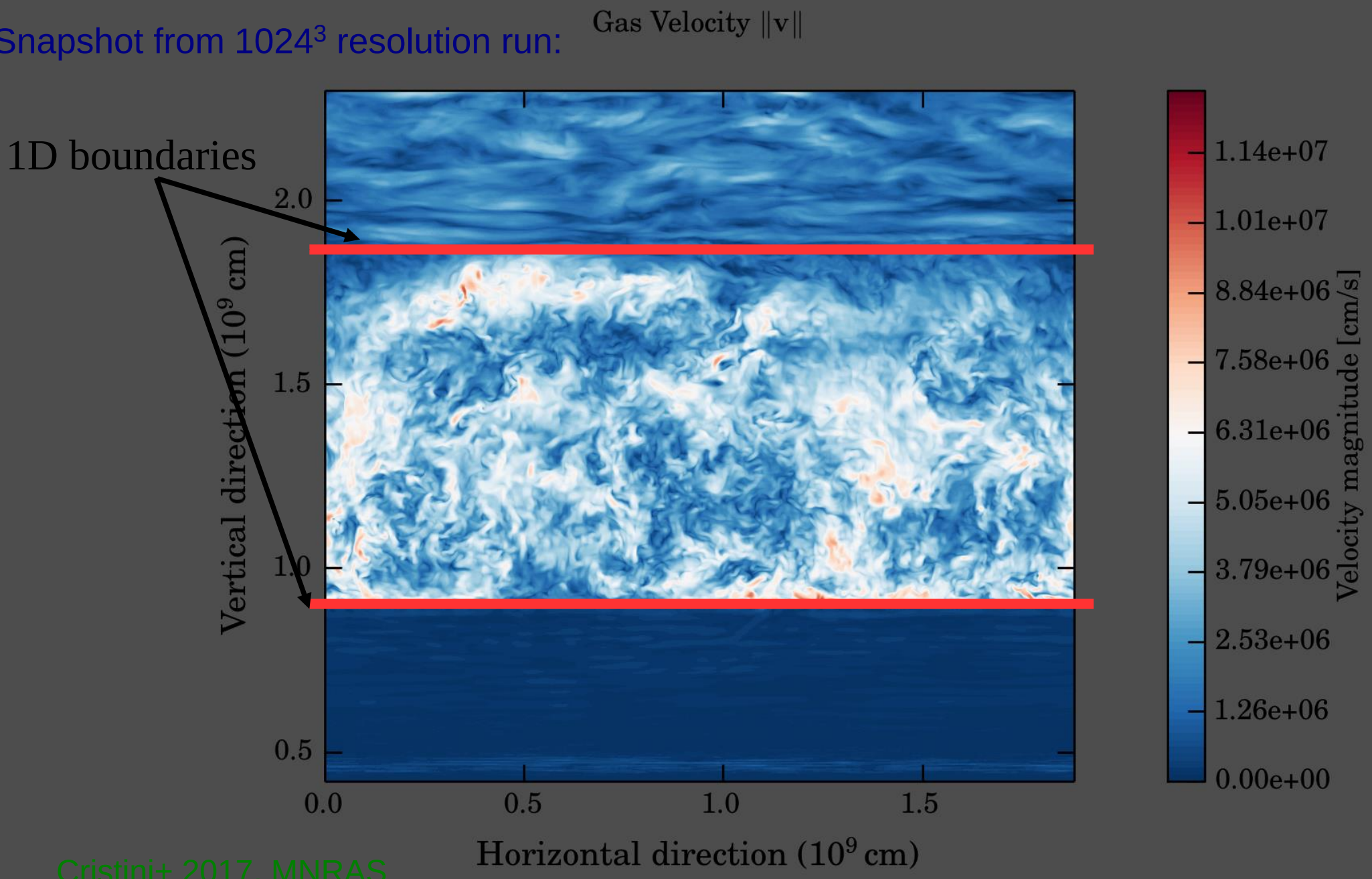

Cristini+ 2017, MNRAS

3D C-shell Simulations: |v| movie

Cristini+ 2017, MNRAS

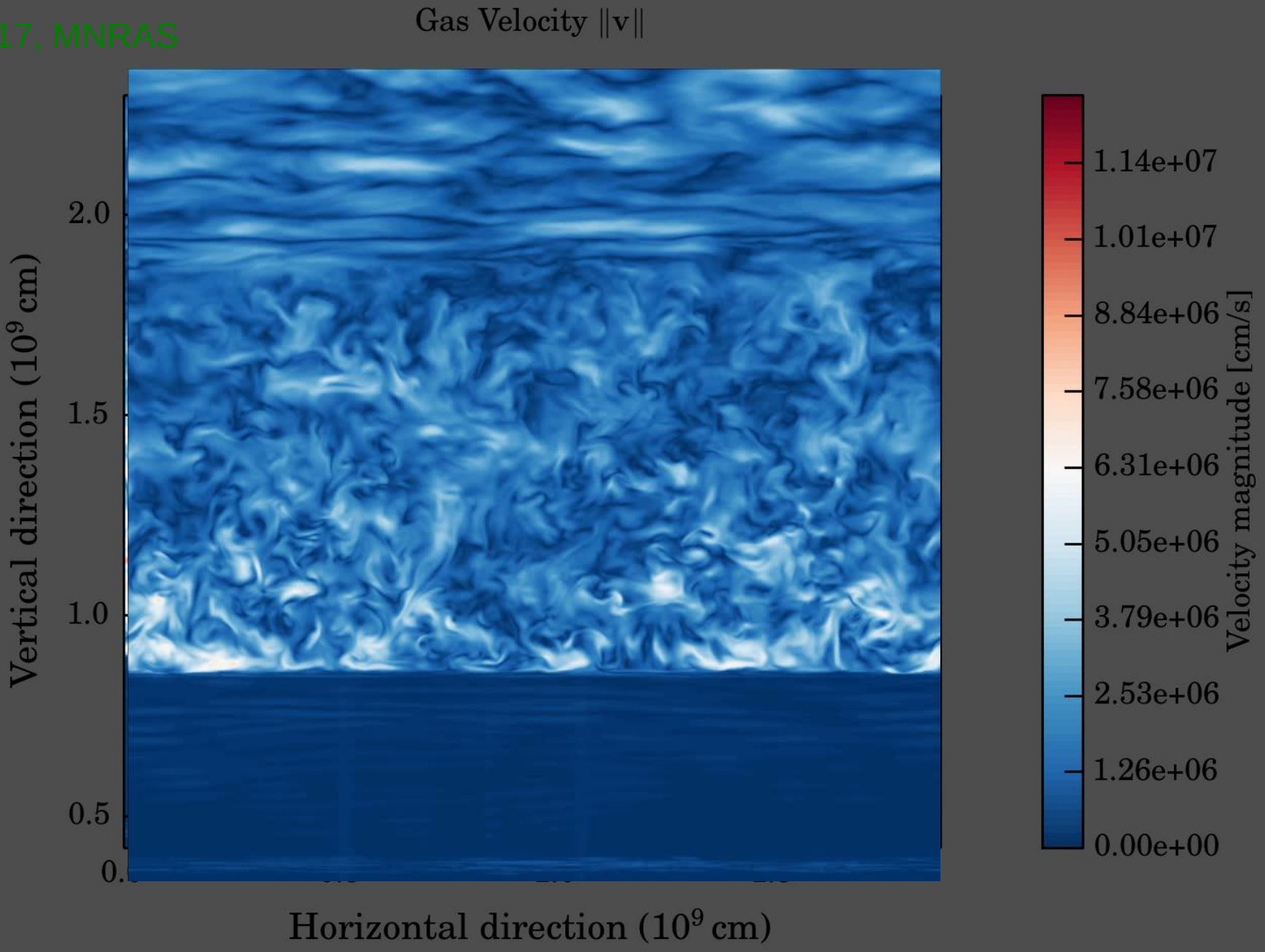

http://www.astro.keele.ac.uk/shyne/321D/convection-and-convective-boundary-mixing/visualisations

3D C-shell Simulations

Snapshot from 1024^3 resolution run:

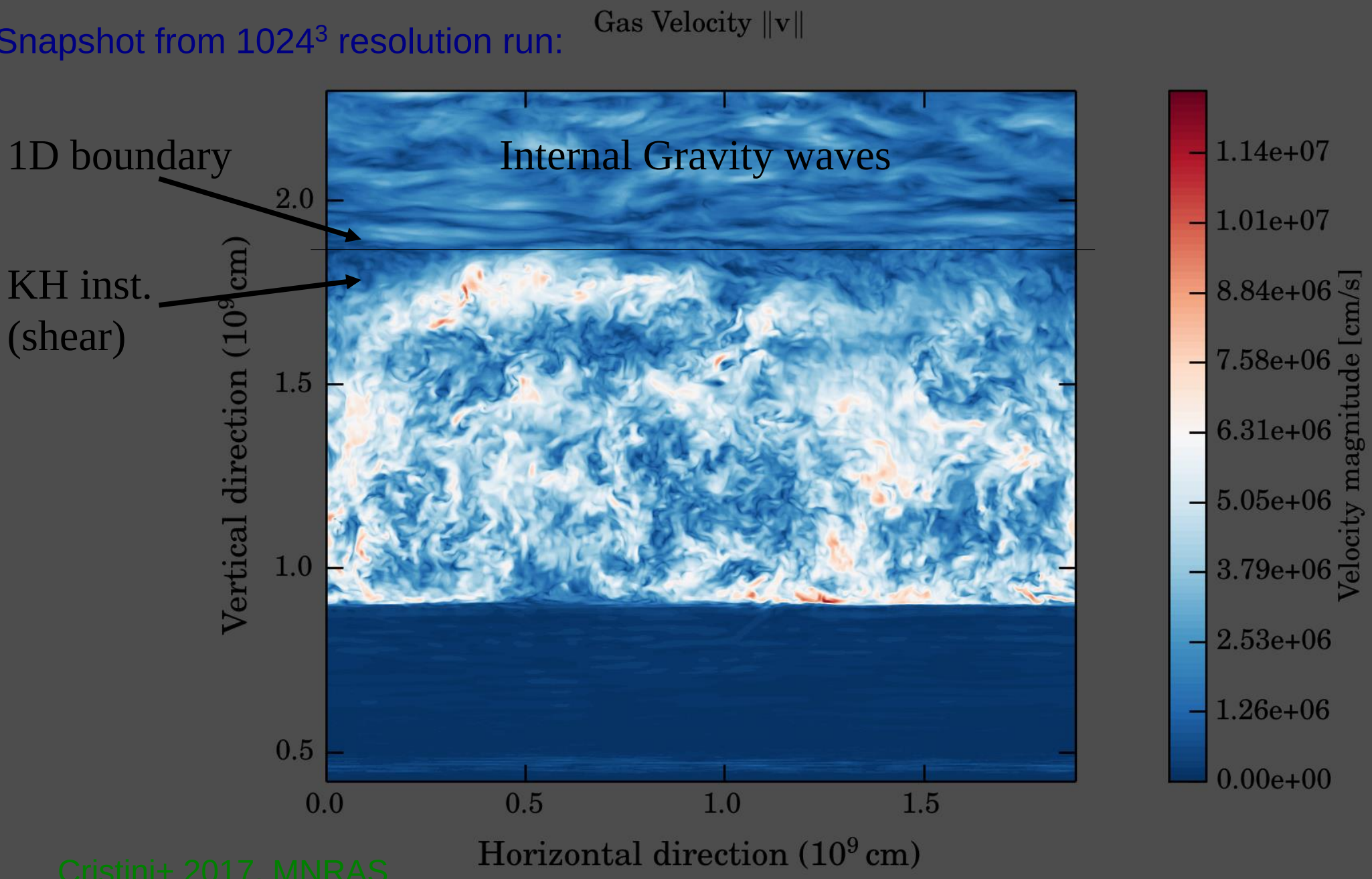

Cristini+ 2017, MNRAS

Resolution & Luminosity Study

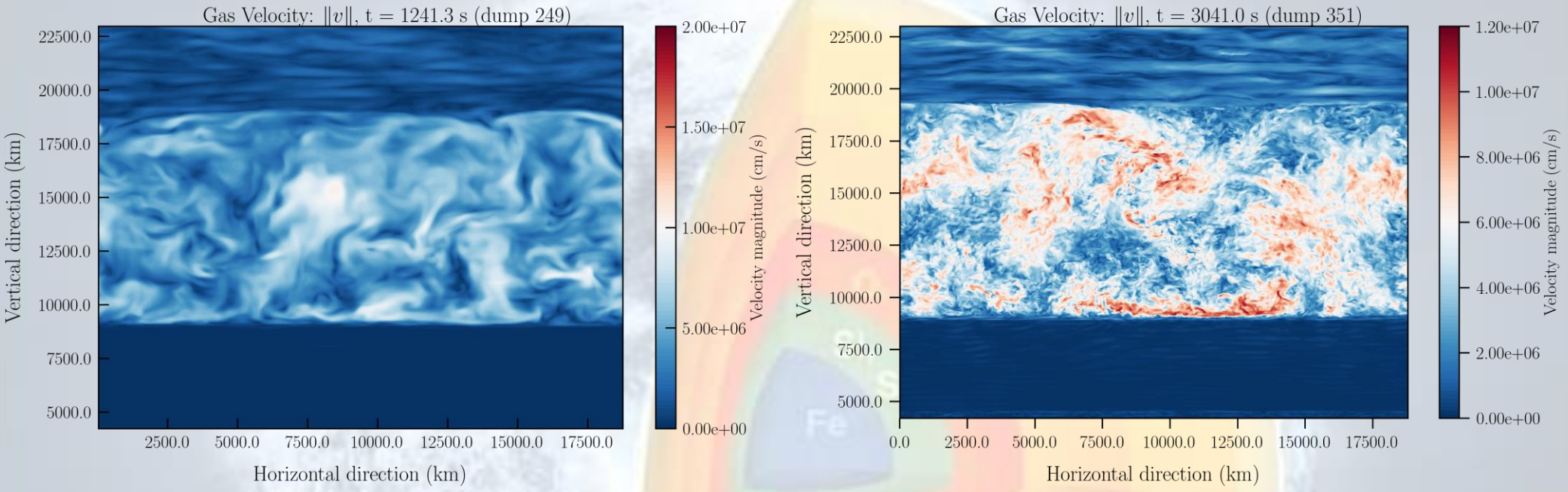

Resolution \ Luminosity	128	256	512	1024
1			eps1	
33			eps33	
100			eps100	
333			eps333	
1000	lrez	mrez	hrez/eps1k	vhrez
3333			eps3k	
10000			eps10k	
33333			eps33k	

Resolution study

Luminosity study

Cristini+2017, MNRAS

Boundary Entrainment

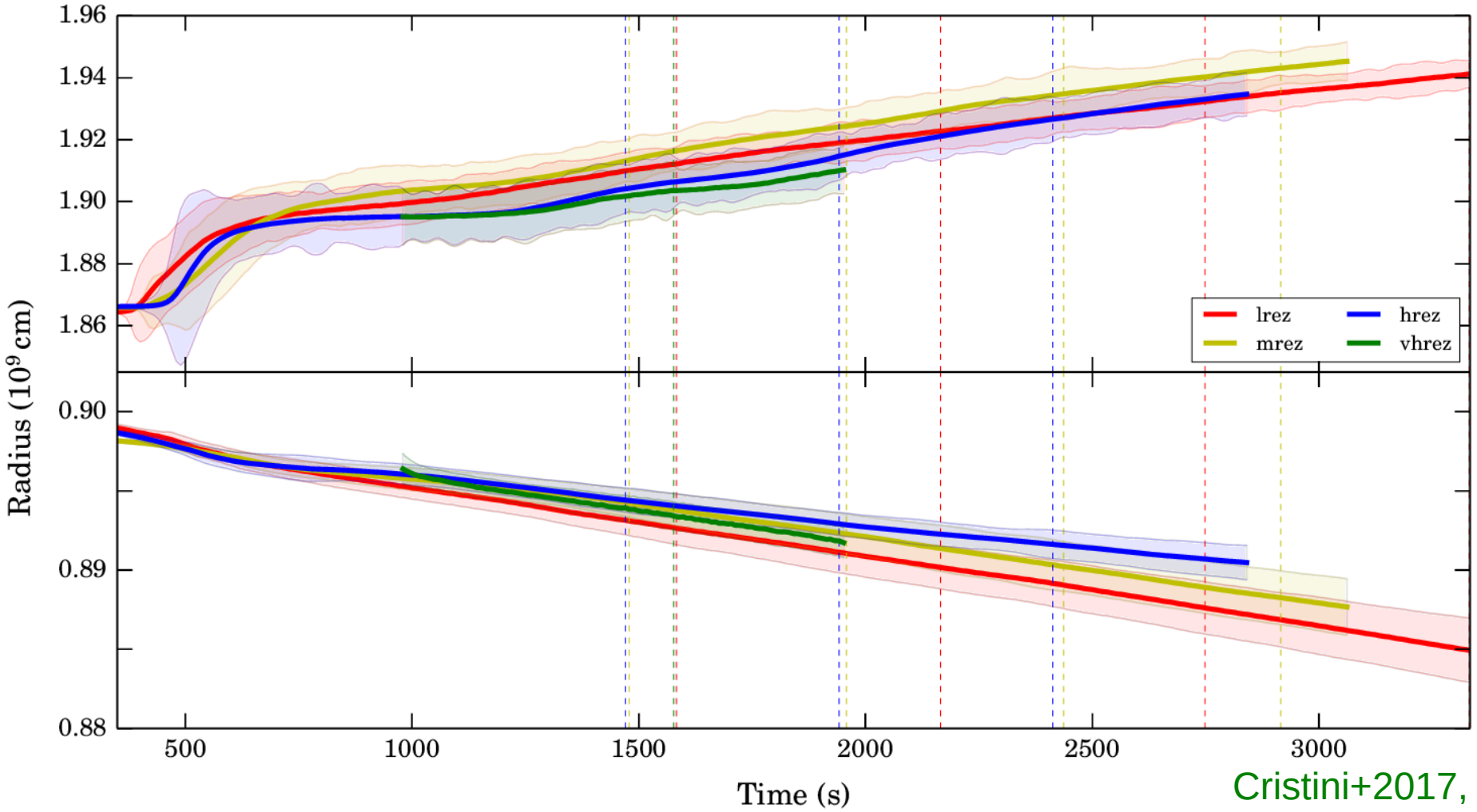

Cristini+2017, MNRAS

Entrainment Law Theory

Cristini et al 2019, MNRAS (see also Garcia & Mellado, 2014, Deardor 1980, Chemel, Staquet and Chollet 2010, Fernando, 1991, Stevens and Lenschow, 2001, Jonker+ 2013)

$$\frac{v_e}{v_c} = ARi_B^{-n},$$

A, n are constants

$$Ri_B = \frac{\Delta B \times l}{v_{rms}^2}$$

$$Ri_B = \frac{stabilising\ potential}{turbulent\ kinetic\ energy}$$

The buoyancy jump is an integral of the squared buoyancy frequency N^2 with respect to radius r, given by

$$\Delta b = \int_{r_1}^{r_2} N^2 \mathrm{d}r, \qquad (2)$$

where r_1 and r_2 encompass the boundary of the convective core, centred at $r = r_b$. The upper limit r_2 is equal to r_b plus some fraction of a pressure scale height; in this study we

A mass entrainment rate, $\dot{M}_{ent}$, can be derived from this to give

$$\dot{M}_{ent} = 4\pi r_b^2 \rho_b v_c A Ri_B^{-n}, \qquad (6)$$

with ρ_b being the density at $r = r_b$. The mass contained within the entrained region, M_{ent}, is then

$$M_{ent} = \sum_j \dot{M}_{ent,j} \Delta t_j \qquad (7)$$

Instantaneous entrainment as in: Staritsin 2013

Cumulative entrainment as in: Scott+ 2021MNRAS.503.4208S

Entrainment Law for C, Ne & O-burning

Cristini et al 2019, MNRAS (see also Garcia & Mellado, 2014, Deardor 1980, Chemel, Staquet and Chollet 2010, Fernando, 1991, Stevens and Lenschow, 2001, Jonker+ 2013)
Georgy+, Rizzuti+, in prep

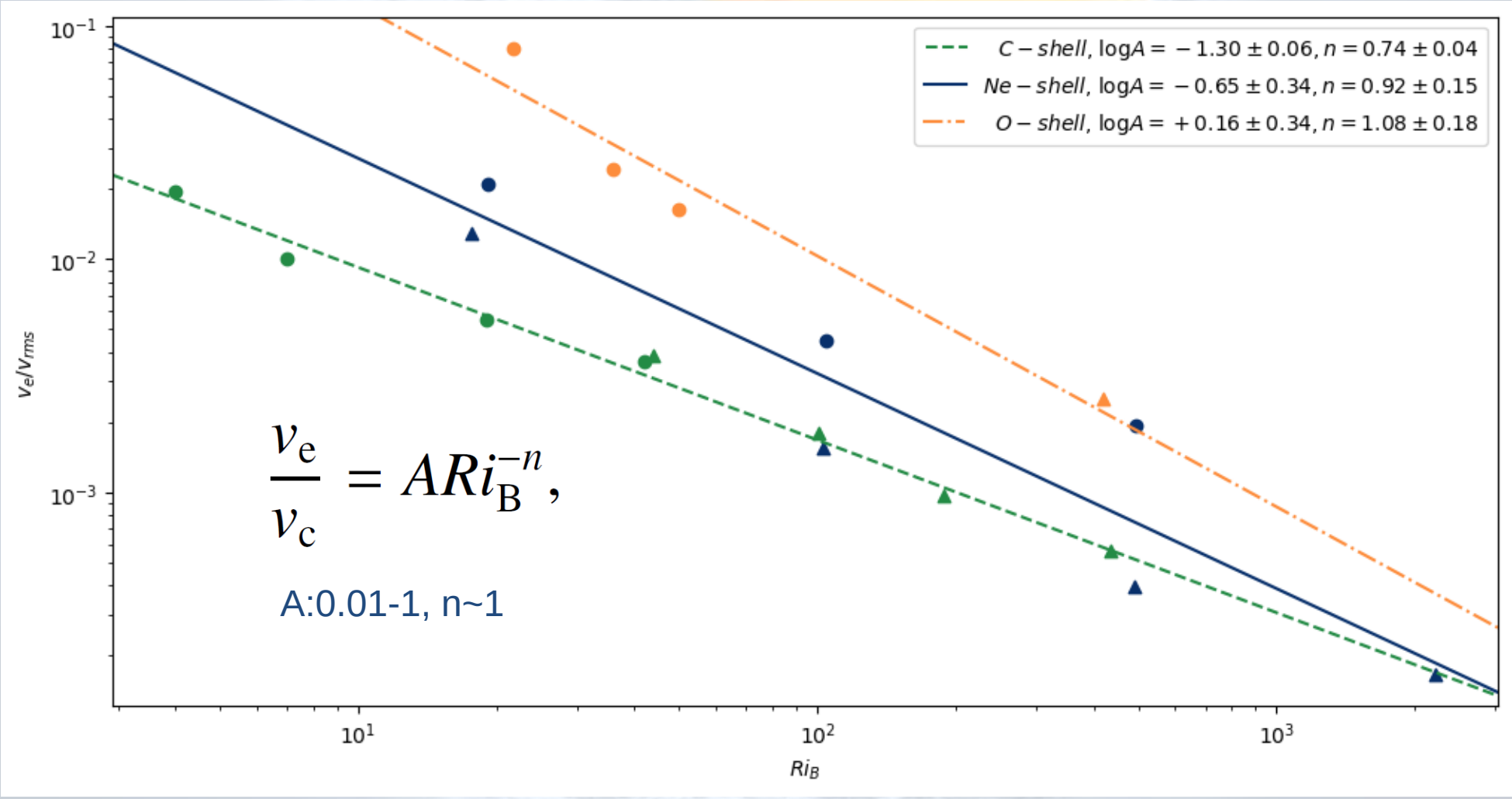

Way Forward: 1 to 3 to 1D link

Targeted 3D simulations

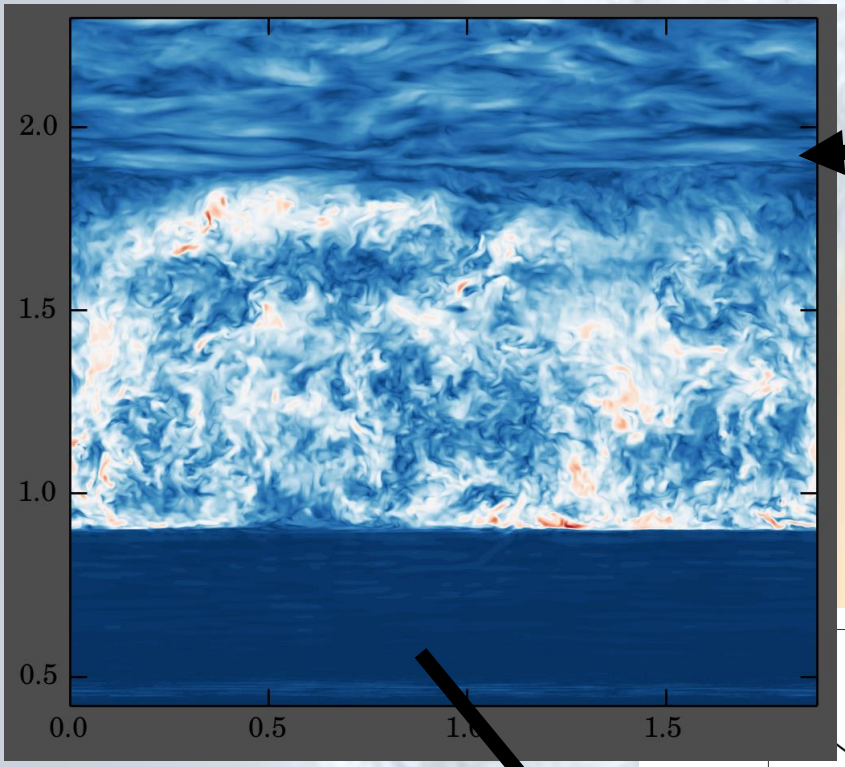

Cristini+2017

Uncertainties in 1D

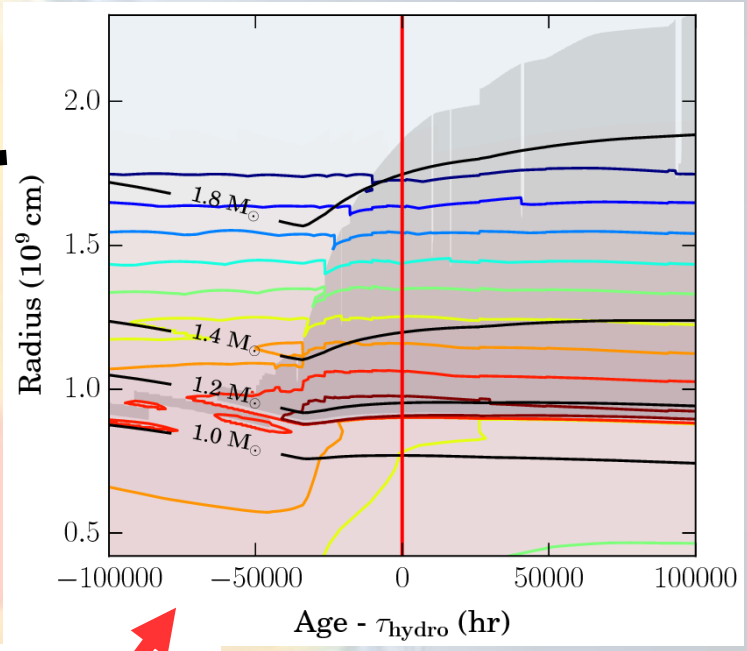

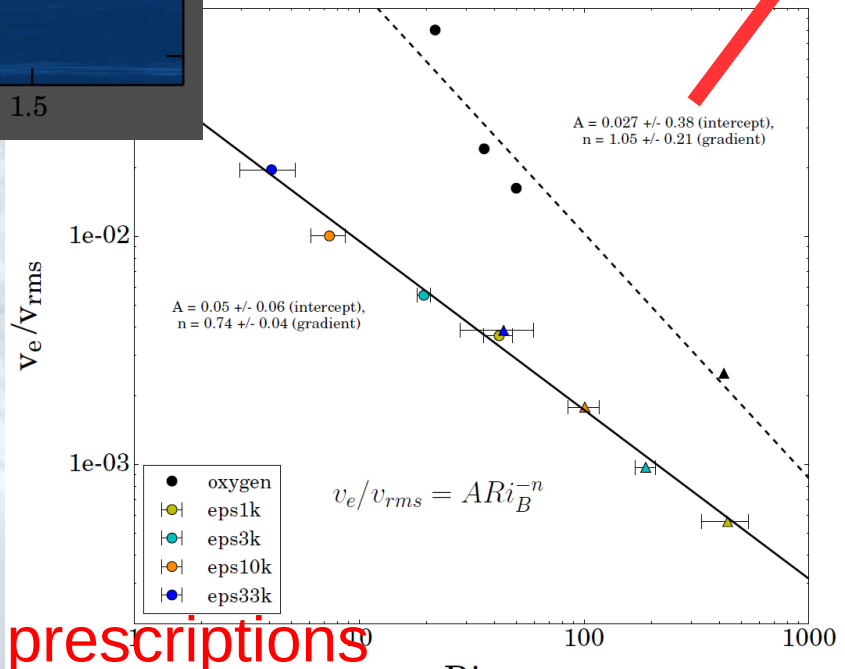

→ Improve theoretical prescriptions

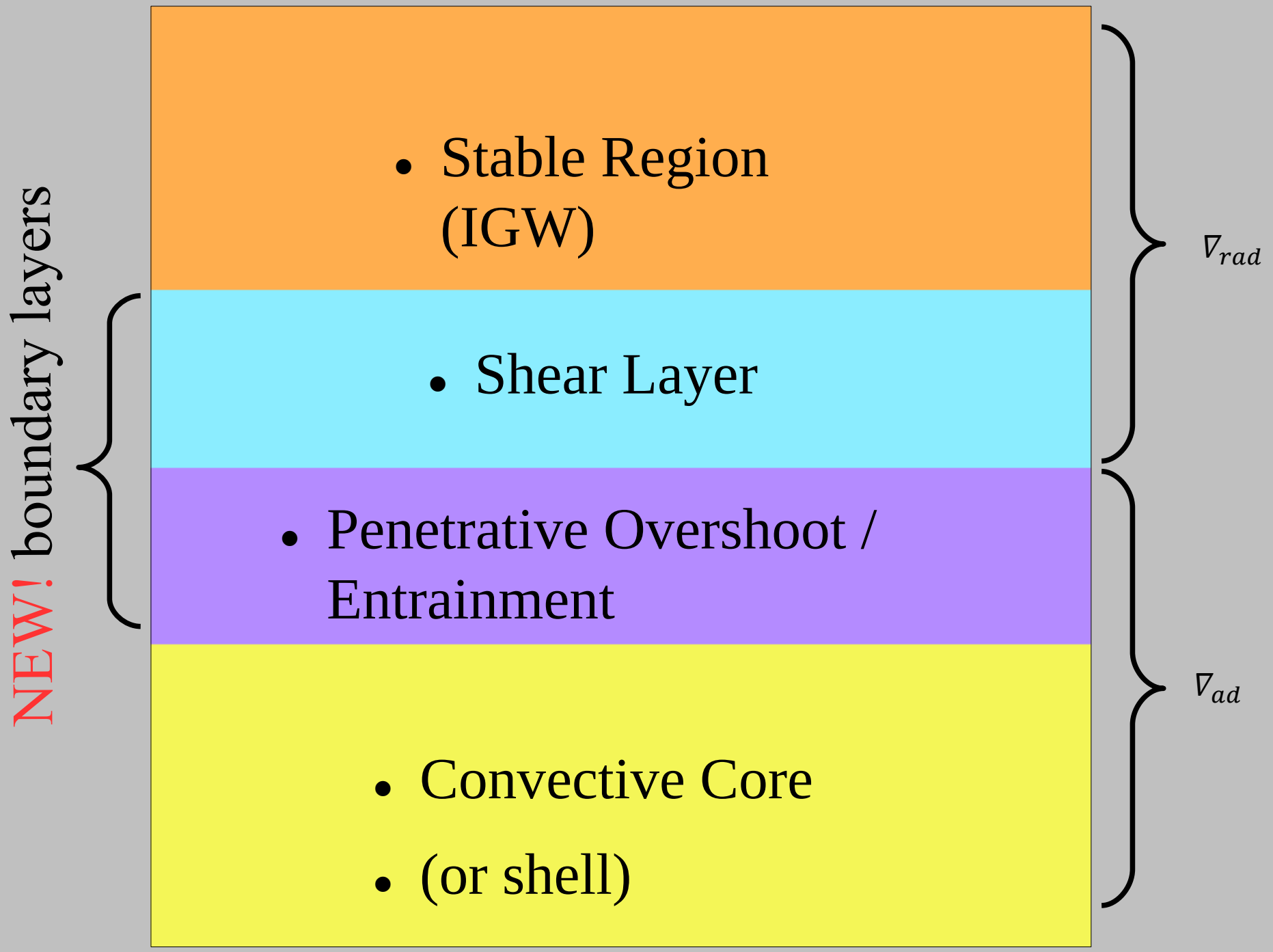
NEW! boundary layers
• Stable Region (IGW)
• Shear Layer
• Penetrative Overshoot / Entrainment
• Convective Core
• (or shell)
∇_{rad}
∇_{ad}

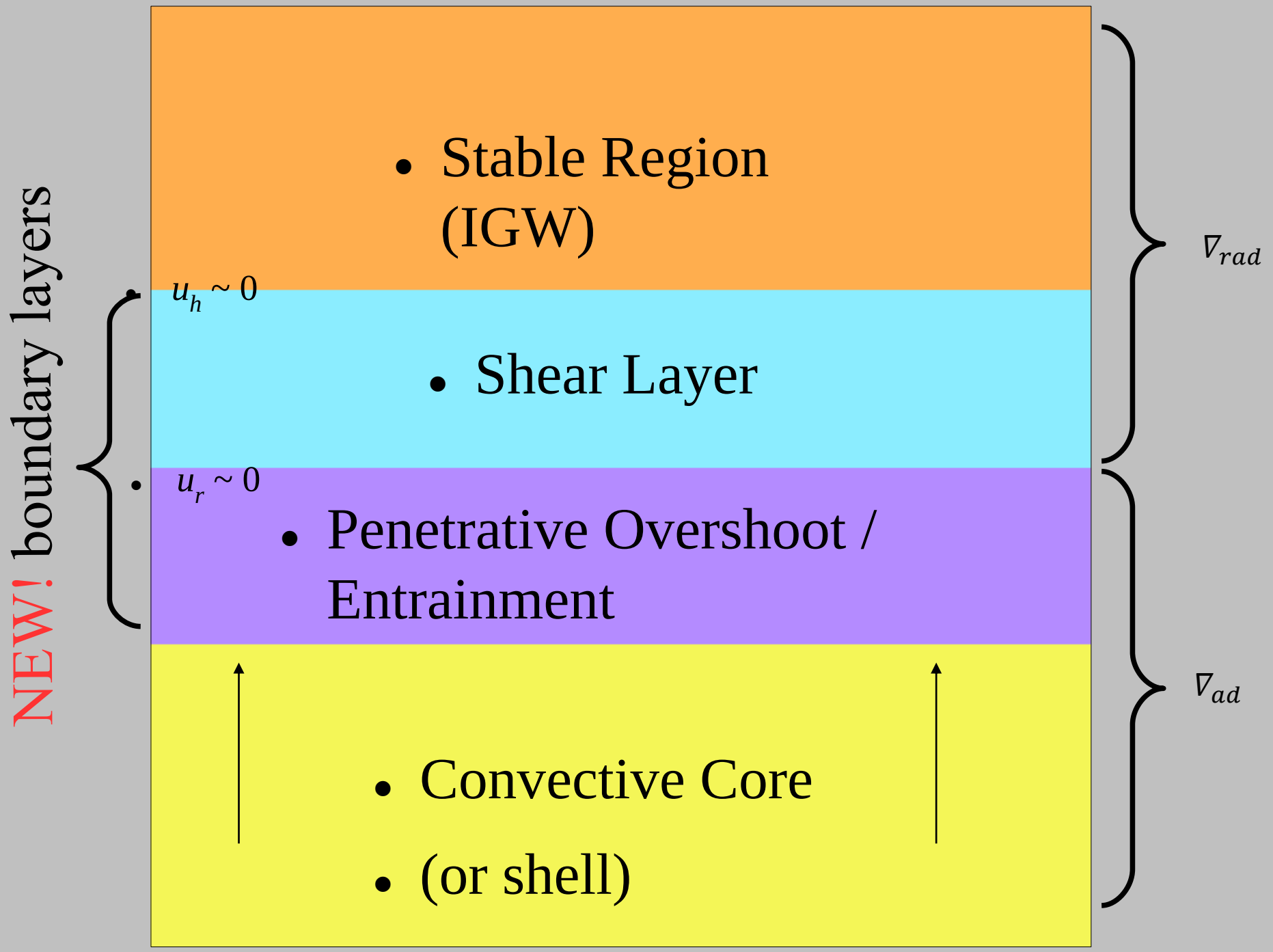
NEW! boundary layers
$u_h \sim 0$
$u_r \sim 0$
• Stable Region (IGW)
• Shear Layer
• Penetrative Overshoot / Entrainment
• Convective Core
• (or shell)
∇_{rad}
∇_{ad}

Implementation of Entrainment in 1D model

Scott+ 2021MNRAS.503.4208S

Calculation of $\Delta b = \int_{r_1}^{r_2} N^2 \mathrm{d}r,$

15 $M_\odot$

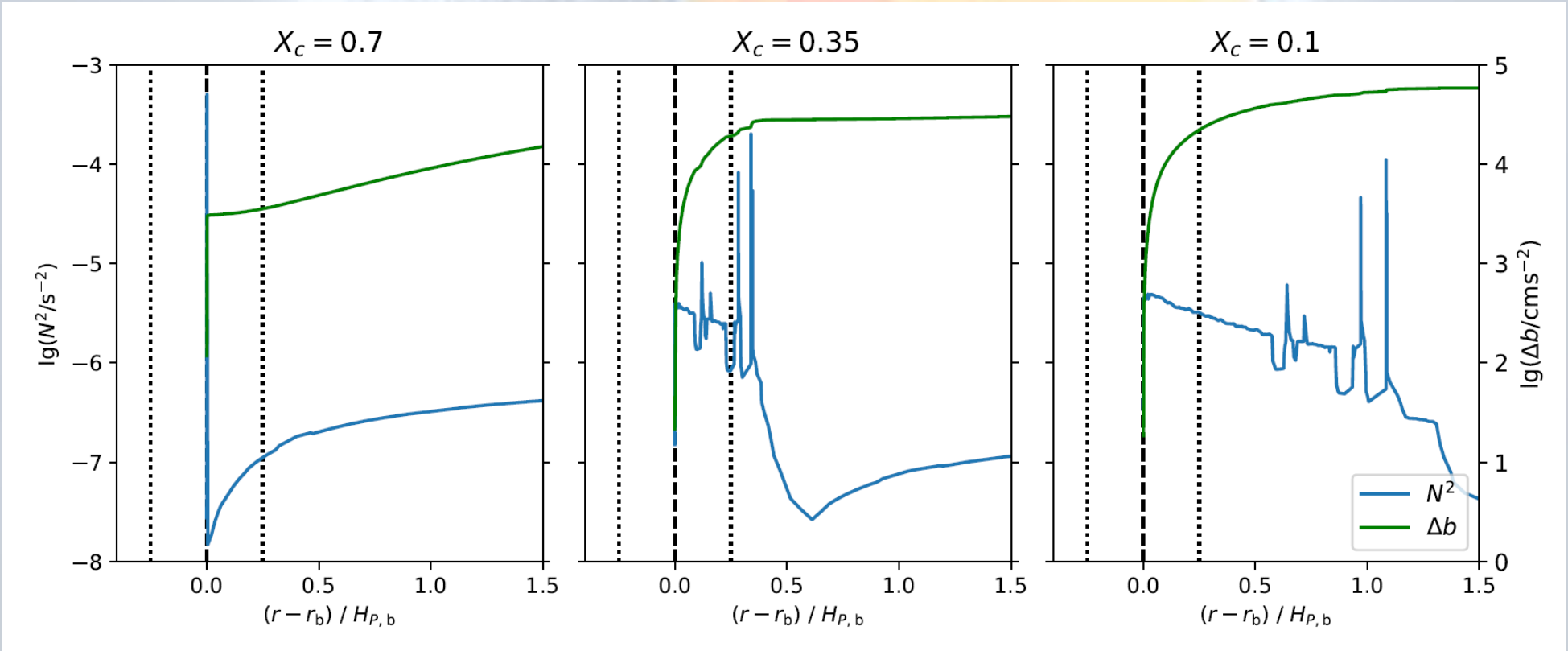

Δb increases with time over MS due to μ-gradient built-up.

Mild dependence of Δb on choice of r_1 and r_2, both chosen to be $H_P/4$

Implementation of Entrainment in 1D model

Scott+ 2021MNRAS.503.4208S

15 $M_\odot$
$A=10^{-4}$
n=1

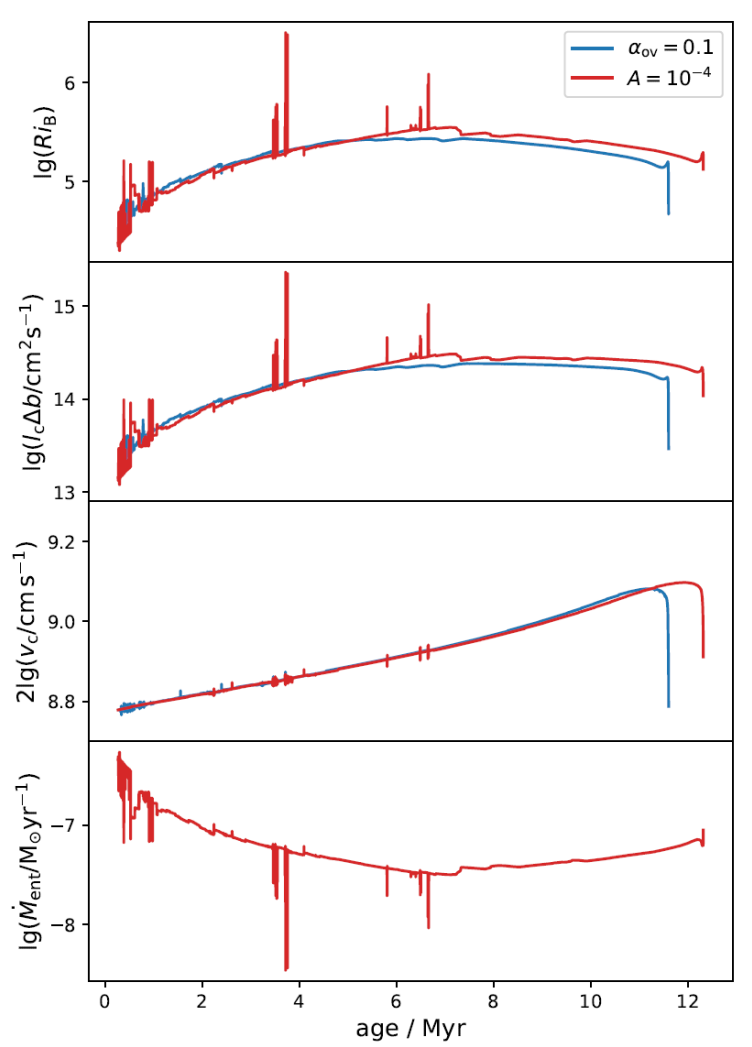

$$Ri_{\mathrm{B}} = \frac{l_{\mathrm{c}} \Delta b}{v_{\mathrm{c}}^2},$$

$$\dot{M}_{\mathrm{ent}} = 4\pi r_{\mathrm{b}}^2 \rho_{\mathrm{b}} v_{\mathrm{c}} A Ri_{\mathrm{B}}^{-n},$$

$$M_{\mathrm{ent}} = \sum_j \dot{M}_{\mathrm{ent},j} \Delta t_j$$

RiB increases with time over MS so entrainment rate decreases

(small change compared to mass dependence)

Boundary Penetrability vs Initial Mass

Scott+ 2021MNRAS.503.4208S

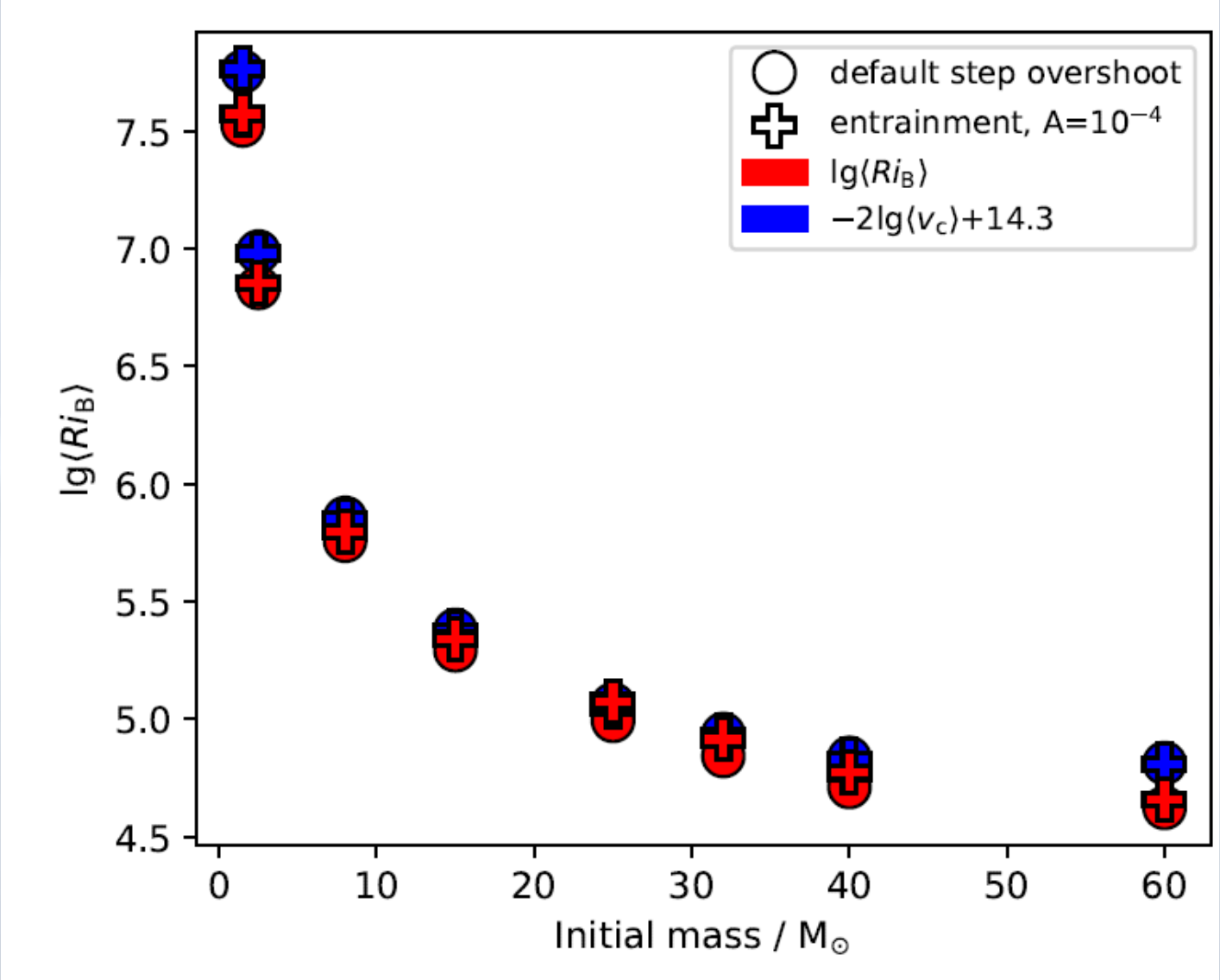

Penetrability (~1/Ri_B) increases with initial mass.

Mainly linked to increase in convective velocity, v_c with mass (Ri_B ~ 1/v_c^2)

Entrainment in 1D model: Impact on MS Width

Scott+ 2021MNRAS.503.4208S

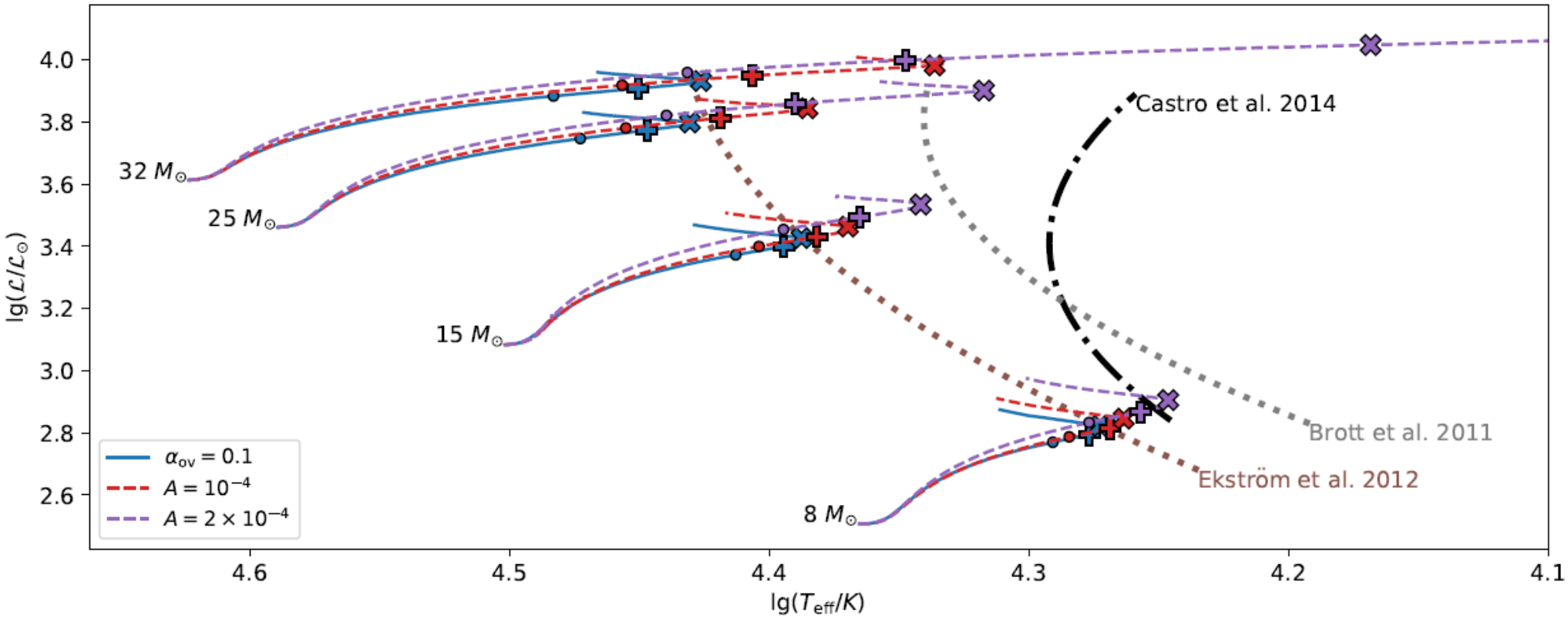

Figure 6. Spectroscopic HRD in the mass range 8 to 32 $M_\odot$ with $\alpha_{ov} = 0.1$ step overshoot and two entrainment models, $A = 10^{-4}$ and 2×10^{-4}. The dotted lines represent the position of the TAMS from model grids with $\alpha_{ov} = 0.1$ (Ekström et al. 2012) and $\alpha_{ov} = 0.335$ (Brott et al. 2011). The dash-dotted line represents the position of the empirical TAMS determined by Castro et al. (2014); see their Table 1 for the polynomial coefficients of the three TAMS lines used in this figure. As in Fig. 3, the dots, pluses and crosses have been placed where the model reaches 90%, 95% and 99% of the MS lifetime respectively.

MS width and its mass dependence better reproduced than current models with a single set of parameters

Entrainment in 1D model: Impact on core masses

Scott+ 2021MNRAS.503.4208S

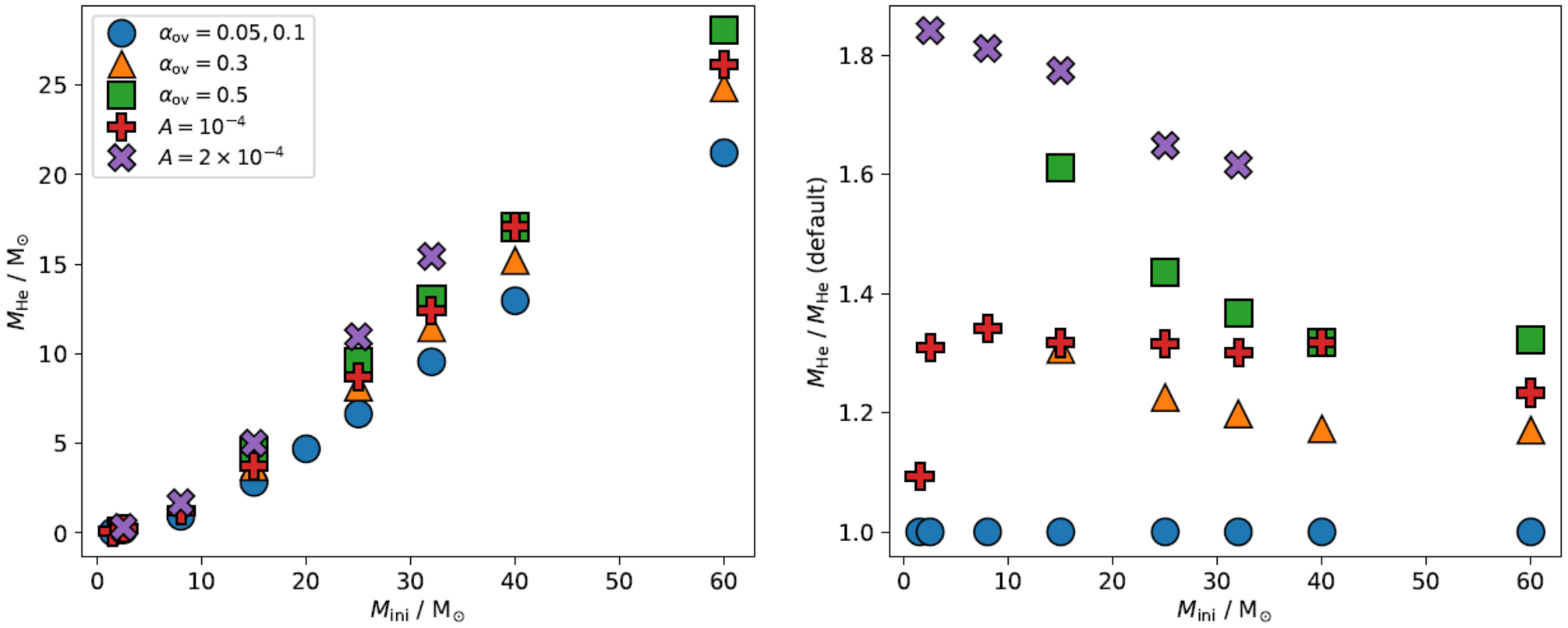

Figure 7. Final helium core mass, M_{He}, for various values of step overshoot α_{ov} and entrainment parameter A. All entrainment models use $n = 1$. Blue circles represent the default value of α_{ov}, which is 0.05 for 1.5 $M_\odot$ and 0.1 otherwise. *Left:* Absolute value of M_{He} against initial mass. The $\alpha_{ov} = 0.1$ point at 20 $M_\odot$ is taken from the Ekström et al. (2012) grid. *Right:* M_{He} normalised by the default step overshoot value.

CO core masses predicted up to 80% larger than for current models: A 15 $M_\odot$ model may behave as a 20-22 $M_\odot$ model.

But A values do not match 3D hydro simulation results yet …

Entrainment in 1D model: "Temporary Fix"

Scott+ 2021MNRAS.503.4208S

Entrainment implementation
Challenging post-MS:

A mass entrainment rate, $\dot{M}_{\rm ent}$, can be derived from this to give

$$\dot{M}_{\rm ent} = 4\pi r_{\rm b}^2 \rho_{\rm b} v_{\rm c} A R i_{\rm B}^{-n}, \quad (6)$$

with $\rho_{\rm b}$ being the density at $r = r_{\rm b}$. The mass contained within the entrained region, $M_{\rm ent}$, is then

$$M_{\rm ent} = \sum_j \dot{M}_{{\rm ent},j} \Delta t_j \quad (7)$$

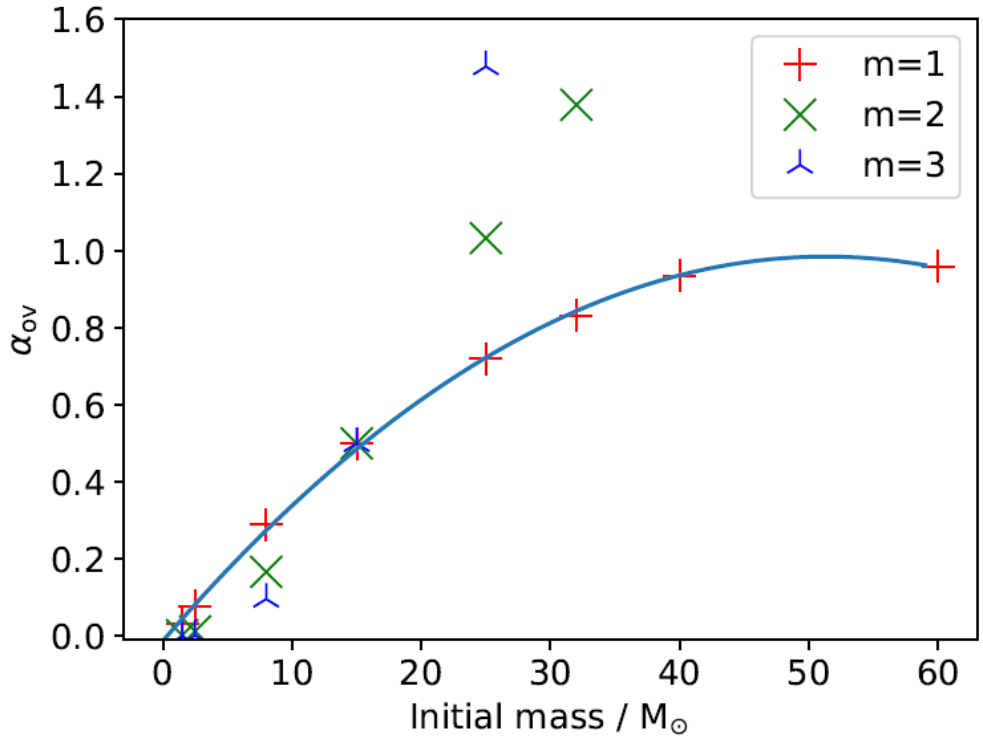

Figure 9. Step overshoot parameter $\alpha_{\rm ov}$ scaled using Eq.8. The polynomial fit to the $m = 1$ points uses the equation $\alpha_{\rm ov}(M_{\rm ini}) = -0.00037867 M_{\rm ini}^2 + 0.03885918 M_{\rm ini} - 0.01237484$. Previous studies such as Claret & Torres (2017) and Moravveji et al. (2016) show that similar results are obtained using an exp-D f parameter which is roughly a factor of 10 to 15 smaller than the equivalent step overshoot $\alpha_{\rm ov}$. Therefore a fit for $f(M_{\rm ini})$ would be roughly 1/10 to 1/15 of $\alpha_{\rm ov}(M_{\rm ini})$.

Mass-dependent α_{ov}/f_{ov} (fits given in caption)

Conclusions & Outlook

- 1 - 3 - 1 D (321D) modelling of stellar interiors:

    - 3D C, Ne, O-shell simulations follow entrainment law

    - Lower boundary stiffer than upper boundary!

- Entrainment law: Implementation difficult but results promising

- More exciting work ahead!

2D Simulations of Convection

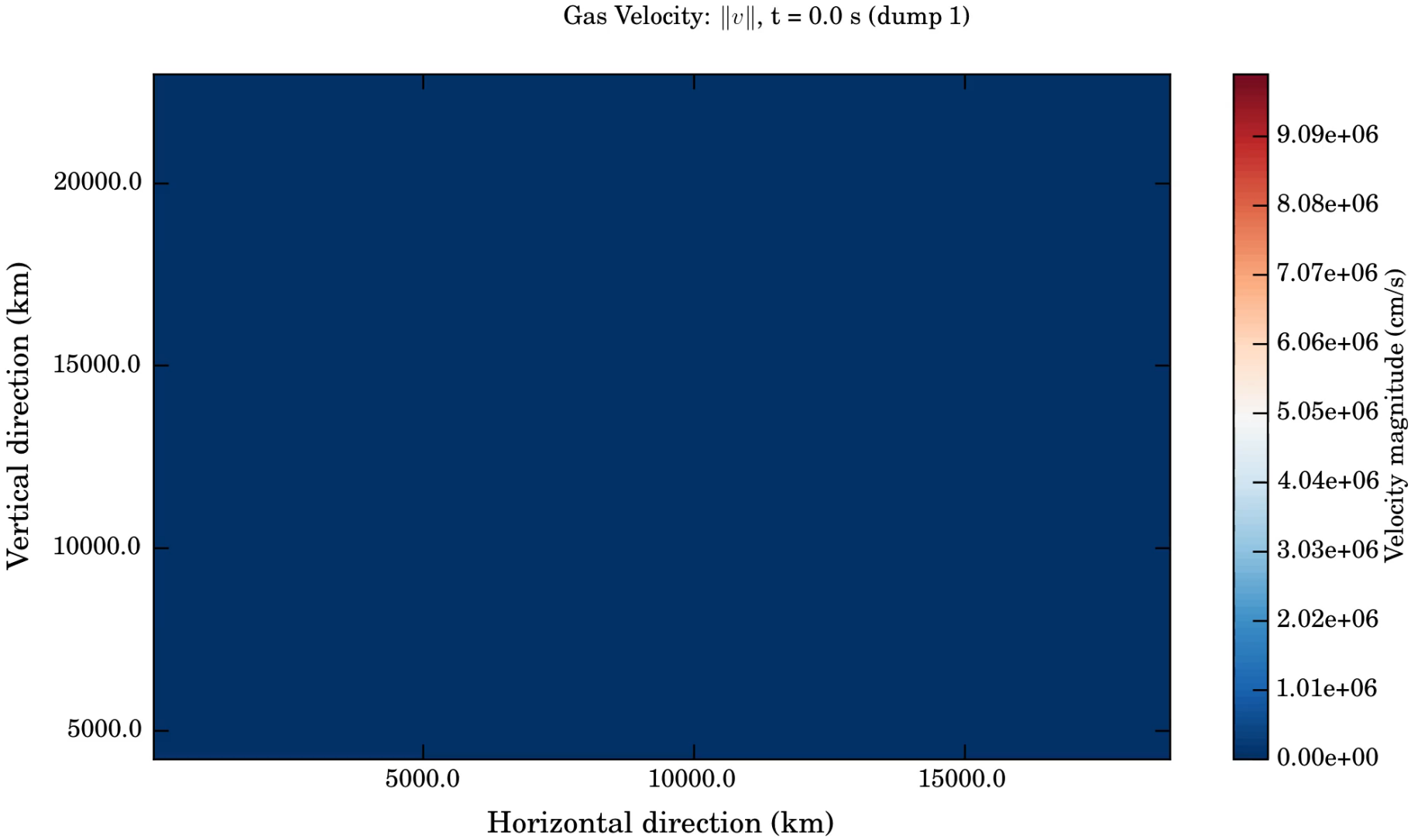

2D simulations a factor of N_z cheaper so 100 – 1000 times cheaper but …
TKE cascade goes upwards rather than downwards!
Vortices survive much longer and merge rather than decay!
Convection is 3D and turbulent so 2D simulations may never reproduce real flow!!

1D Model Uncertainties: MS Width

sHRD: Castro et al (2014A&A...570L..13C),
Langer & Kudritzki (2014, A&A, 564, A52)

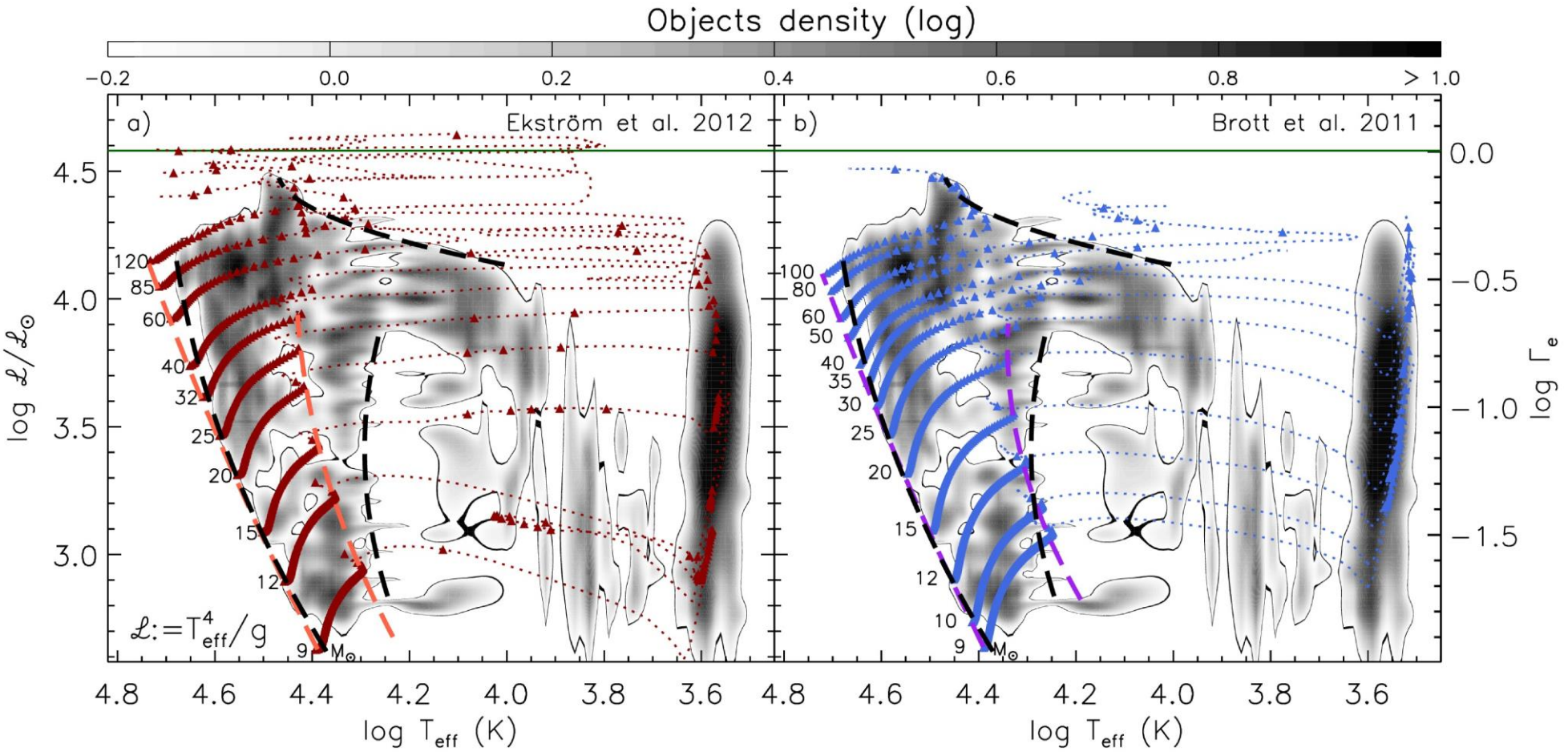

MS width and its mass dependence not reproduced by current models

(but see Vink et al. 2010;McEvoy et al. 2015)

1D Model Uncertainties: L-M Plane

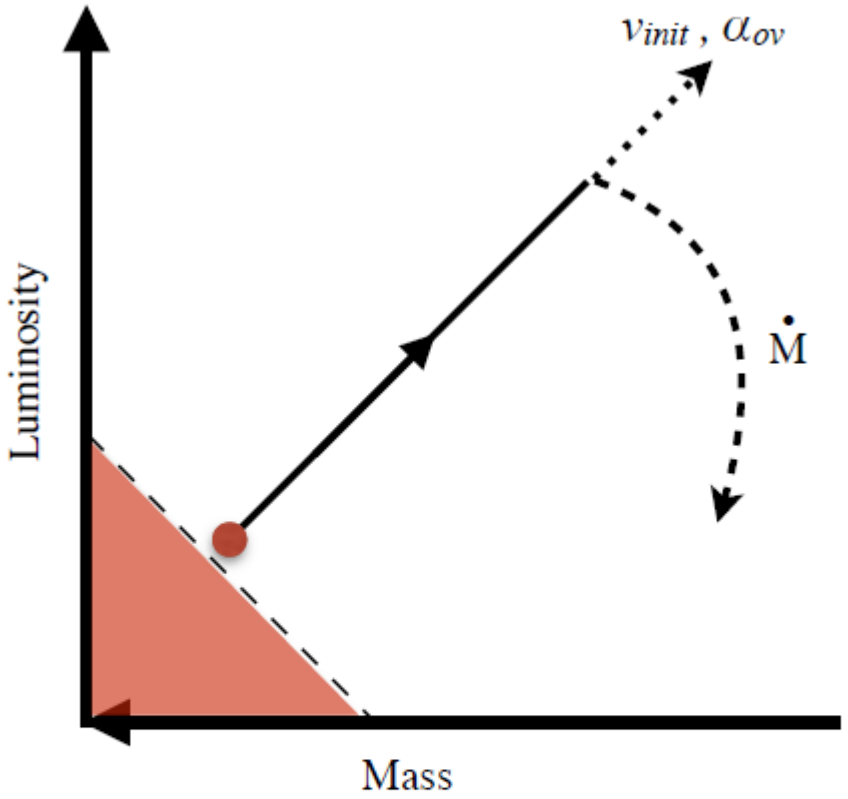

Fig. 4. Illustration of the mass-luminosity plane with a typical evolutionary track entering the ZAMS at the red dot, evolving along the black arrow. The dotted vector suggests how increased rotation and/or convective overshooting may extend the $M-L$ vector. The curved dashed line represents the gradient at which mass-loss rates affect this $M-L$ vector. The red solid region represents the boundary set by the mass-luminosity relationship, and as such is forbidden.

Higgins & Vink (A&A 622, A50, 2019)

α_{ov} up to 0.5 H_P and

rotation-induced mixing

both needed to explain

HD166734

See also Martinet et al 2021, A&A

α_{ov} up to 0.5 H_P ; f_{ov} up to 0.05 from Asteroseismology

See e.g. Deheuvels et al. 2016, Aerts et al 2018, Claret & Torres 2019, Pedersen et al 2020, 2021; Aerts et al ...

1D Model Uncertainties: Post-MS

Martins and Palacios (2013)

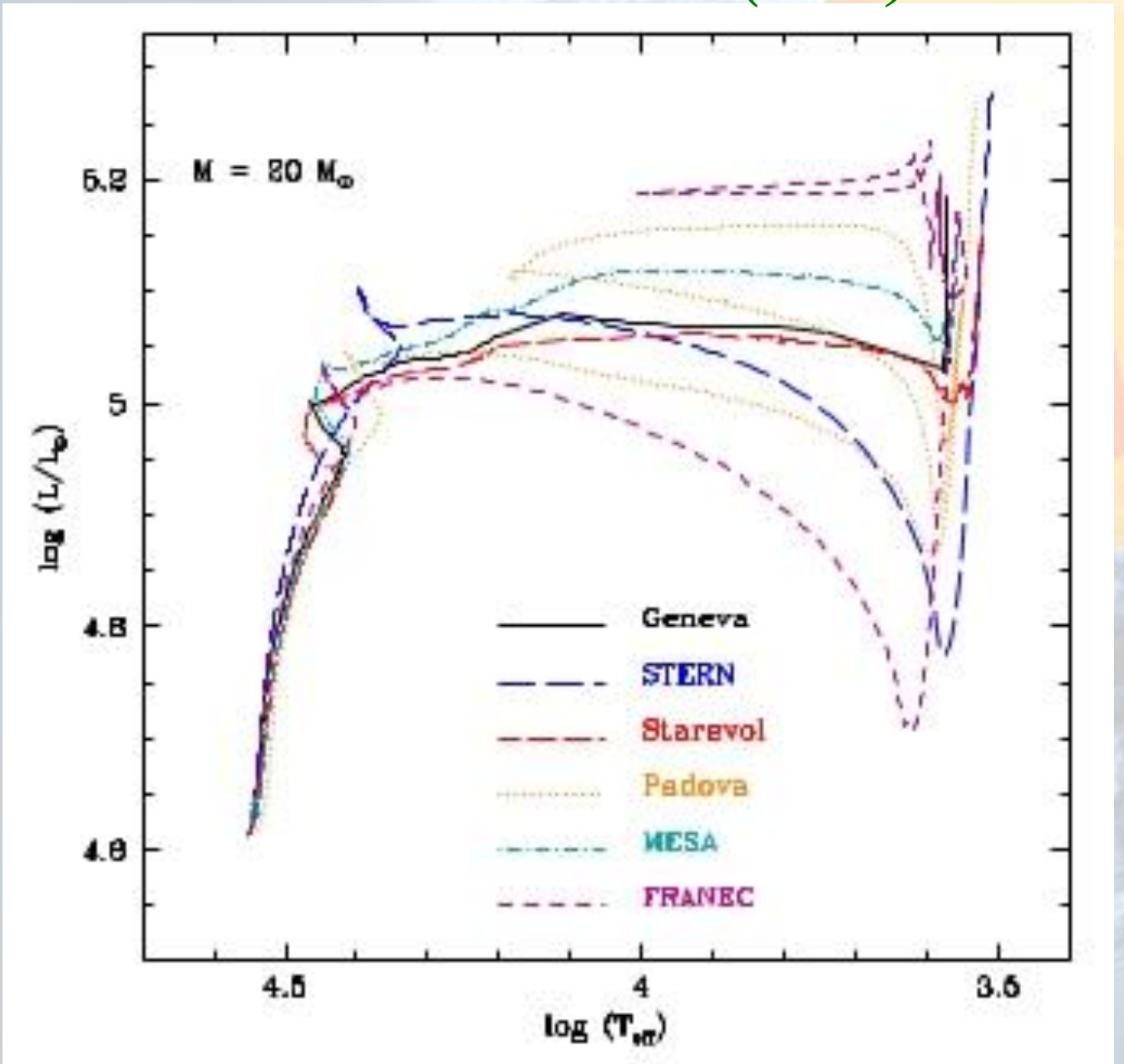

Different prescriptions for convective mixing and free parameters strongly affect post-MS evolution.

See also Georgy+2014,A&A

Jones et al 2015, MNRAS, 447, 3115

1D Model Uncertainties: Core Masses

Kaiser et al, MNRAS 496, 1967 (2020)

Table 2. The absolute and relative variation of the total mass, M_{tot}, the helium core mass, M_{α}, and the carbon-oxygen core mass, M_{CO}. The individual values of each model are shown in Table 1. The values include *Ledoux* and *Schwarzschild* models.

	ΔM_{tot} ($M_{\odot}$)	δM_{tot}	ΔM_{α} ($M_{\odot}$)	δM_{α}	ΔM_{CO} ($M_{\odot}$)	δM_{CO}
15 $M_{\odot}$	3.38 (3.45)	27.72% (27.80%)	2.30 (2.74)	43.07% (51.31%)	2.40 (3.94)	69.77% (114.53%)
20 $M_{\odot}$	8.60	74.35%	2.94	36.70%	2.94	51.49%
25 $M_{\odot}$	9.02	65.84%	3.96	40.08%	4.1	55.48%

Notes. The variation for a quantity Q is calculated as $\delta Q = \frac{\Delta Q}{Q_{ref}} \equiv \frac{Q_{max} - Q_{min}}{Q_{ref}} \times 100$, where Q_{max} and Q_{min} are the maximal and minimal values of the quantity for the initial mass and Q_{ref} the value of the reference model (see the text).

* The values in parentheses include the models with no CBM.

Up to 70% uncertainties in CO core masses predicted by models using the full range of CBM parameters. A 15 $M_{\odot}$ model may behave as a 20 $M_{\odot}$ model.

1D Model Uncertainties: BH-mass gap

e.g. Farrel et al, MNRAS (2020) & references therein

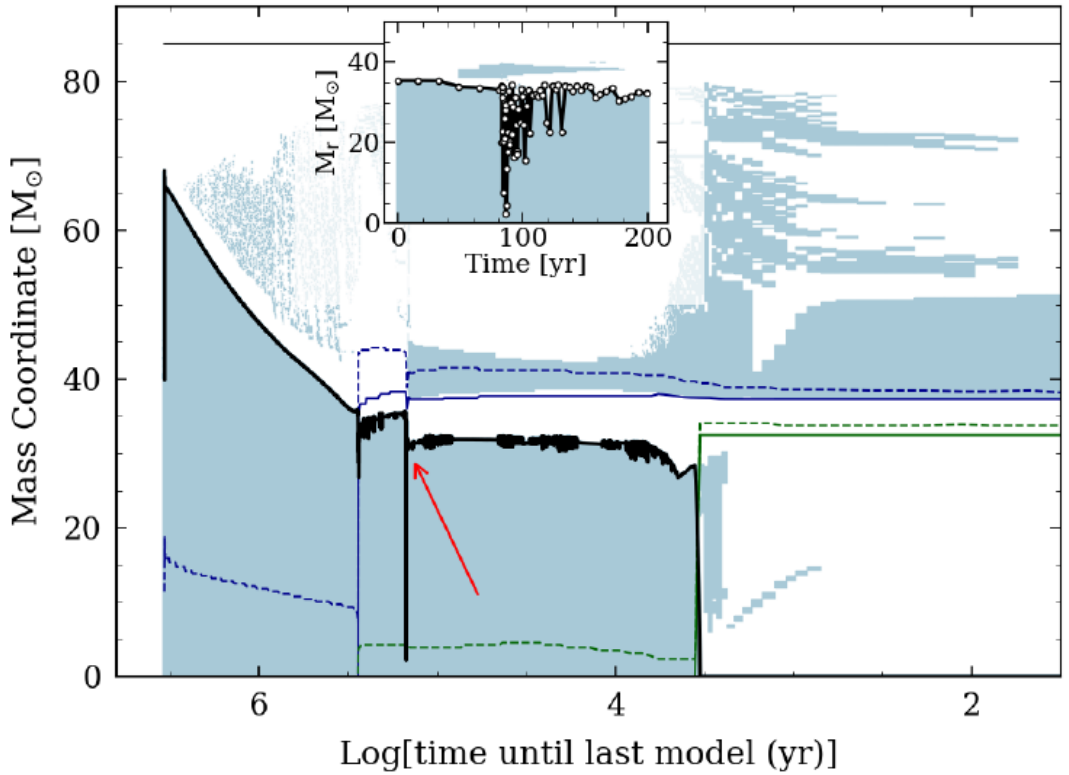

Figure 2. Kippenhahn diagram of a GENEC non-rotating 85 $M_\odot$ model at $Z = 0$. Solid (dashed) lines correspond to the peak (100 erg/g/s) of the energy generation rate for H burning (blue) and He burning (green). The red arrow indicates the H-He shell interaction. An inset is included at the top of the figure to show that the interaction is resolved, where white circles indicate each timestep.

Shell mergers/interactions reduce CO-core mass at very low Z.

1D Model Uncertainties: Post-MS

Detailed convective shell history affects fate of models: strong/weak/failed explosions!!!

Sukhbold & Woosley, 2014ApJ...783...10S

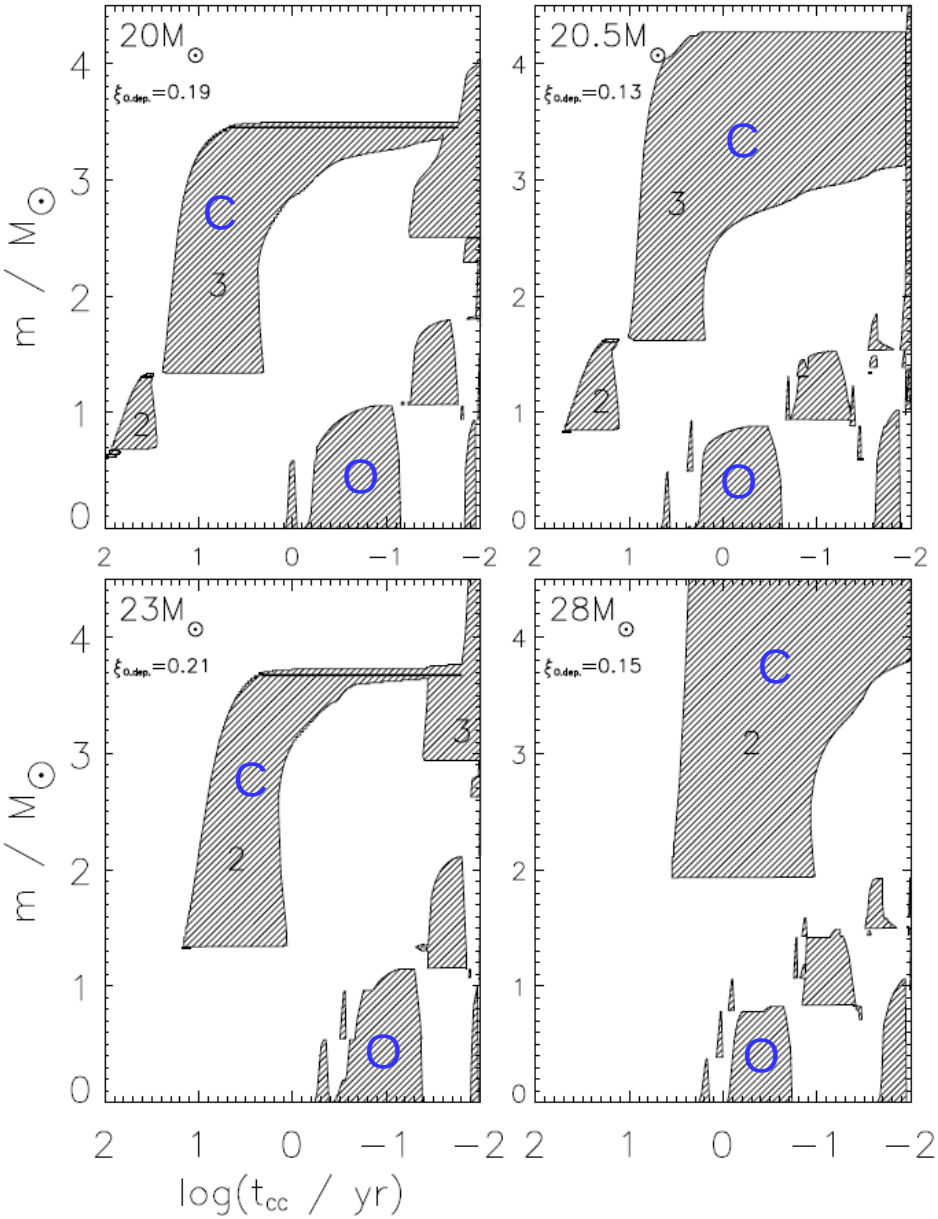

FIG. 13.— Convective history of four models showing the major

Sukhbold, Ertl et al, 2016ApJ...821...38S,
Ugliano et al 2012, Ertl et al 2015

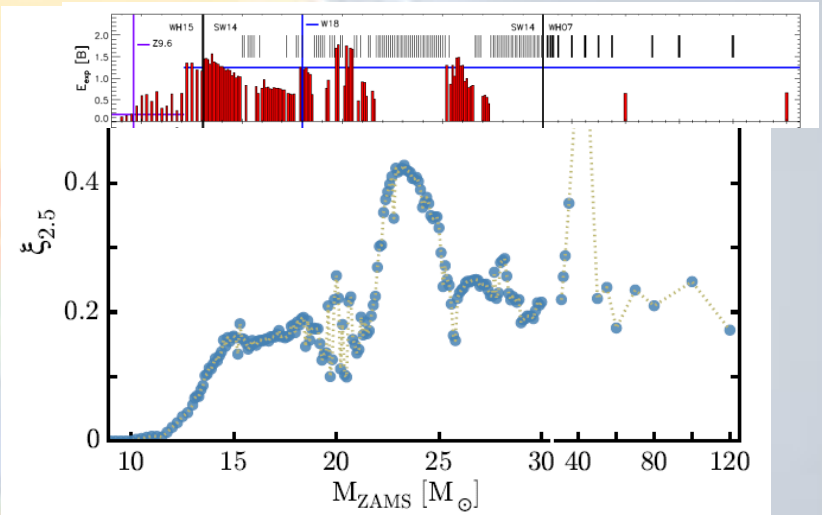

FIG. 1.— The compactness parameter, $\xi_{2.5}$, (eq. (1); O'Connor & Ott 2011) characterizing the inner 2.5 $M_\odot$ of the presupernova star is shown as a function of zero-age main sequence (ZAMS) mass for all 200 models between 9.0 and 120 $M_\odot$. The compactness

Non-monotonic behaviour?

We are particularly interested in how the "explodability" of the presupernova models and their observable properties correlate with their "compactness" (Fig. 1; O'Connor & Ott 2011)

$$\xi_M = \frac{M/M_\odot}{R(M)/1000\,\mathrm{km}}\Big|_{t_{\mathrm{bounce}}}, \qquad (1)$$

and other measures of presupernova core structure (§ 3.1.3;Ertl et al. (2015)). Using a standard central engine in presupernova models of variable compactness, a significant correlation in outcome is found (§ 4). As pre-